RSC Advances

PAPER

View Article Online
View Journal | View Issue

Cite this: *RSC Adv.*, 2017, **7**, 55620

Cu^{2+}-catalyzed and H_2O_2-facilitated oxidation strategy for sensing copper(II) based on cysteine-mediated aggregation of gold nanoparticles†

Yingjie Ye,[a] Qian Zhang,[a] Fei Wang,[a] Yue Li,[a] Fengxian Gao[a] and Yongxing Zhang*[b]

Received 1st September 2017
Accepted 4th December 2017

DOI: 10.1039/c7ra09750f

rsc.li/rsc-advances

As an essential element, copper ions (Cu^{2+}) play important roles in human beings for their participation in diverse metabolic processes, as a cofactor or a structural component of enzymes. However, excessive uptake of Cu^{2+} gives rise to the risk of certain diseases. Then it is important to develop simple ways to monitor and detect Cu^{2+}. In this study, a facile colorimetric sensor for the sensitive determination of Cu^{2+} was developed based on the Cu^{2+}-catalyzed oxidation of cysteine by H_2O_2 to cystine, a process that prohibits the cysteine-triggered aggregation of the Au nanoparticles (AuNPs) stabilized by polyethylene glycol (PEG). With this strategy, the concentration of Cu^{2+} could be detected with the naked eye or with ultraviolet-visible spectroscopy, and the limits of detection for Cu^{2+} were 250 nM and 50 nM, respectively. Additionally, the proposed method shows excellent anti-interference capability against many other metal ions, and in real water samples.

1. Introduction

Copper, an important cofactor or a structural component of many enzymes and other proteins in living organisms, is an essential and significant micronutrient for biological functions. However, the accumulation of copper in organisms may lead to adverse effects, including gastrointestinal distress, liver or kidney damage, and serious neurodegenerative diseases.[1,2] As a result of its widespread application in agriculture and industry, copper continues to be one of the major components of environmental pollutants. Therefore, it is particularly important to establish practical and efficient technologies for rapid determination of copper ions with high sensitivity and selectivity.

Some analytical techniques, such as electrochemical sensors,[3,4] fluorescence sensors,[5,6] atmospheric pressure X-ray photoelectron spectroscopy (XPS),[7] plasma mass spectrometry,[8] surface-enhanced Raman spectroscopy,[9] quantum-dot-based assays[10,11] and colorimetric sensors[12,13] have been developed for the detection of Cu^{2+}. Colorimetric methods are convenient and effective in many applications because the readout requires only human eyes, without the aid of any sophisticated instruments. In the last few decades, plasmonic nanoparticles, especially gold nanoparticles (AuNPs), have attracted much attention as an ideal transducer of colorimetry for sensing, recognizing, and determination of ions and small biomolecules because the aggregation of solutions with low concentrations of AuNPs displays a clear color change.[14–16] AuNPs-based colorimetric methods can also be applied to detect Cu^{2+}.

Copper could be used as catalysts in some reactions, and the amount of copper needed for completion of the reaction is typically small. Therefore, some methods based on color changes of AuNPs arising from copper-catalyzed reactions have been developed for the detection of trace amounts of Cu^{2+}. For example, Jiang *et al.*[17] reported a method for the detection of Cu^{2+} ions by azide- and terminal alkyne-functionalized AuNPs in aqueous solutions using click chemistry, and they extended this method for the colorimetric detection of immunoassays.[18] Recently, Cu^{2+} has been reported to act as catalysts for oxidative transformation of thiol groups to disulfide bonds in the presence of O_2.[19,20] The change between the dispersion/aggregation states of AuNPs could be controlled by thiols with the aid of Cu^{2+} and O_2, so that the colorimetric detection of Cu^{2+} could be realized.[21,22] However, it is a relatively slow process that the Cu^{2+}-catalyzed oxidation of thiol groups to disulfide bonds in the presence of dissolved O_2. So the detection of Cu^{2+} is time-consuming at room temperature.[19,22] To increase the rate of reaction, the detection needed to be performed at a relatively high temperature.[21] Therefore, it is necessary to establish a fast, sensitive, and convenient method for the determination of Cu^{2+}.

[a]*Department of Materials and Chemical Engineering, Henan Institute of Engineering, Zhengzhou, Henan 451191, P. R. China*

[b]*School of Physics and Electronic Information, Huaibei Normal University, Huaibei, Anhui 235000, P. R. China. E-mail: zyx07157@mail.ustc.edu.cn; Tel: +86 561 3803394*

† Electronic supplementary information (ESI) available. See DOI: 10.1039/c7ra09750f

Herein, we presented a simple and reliable colorimetric strategy using cysteine-induced aggregation of AuNPs as a highly efficient signal amplification method based on the catalytic property of Cu^{2+} in the presence of H_2O_2. According to a previous report, cysteine can bind to the surface of AuNPs through the formation of Au–S bonds. Because the carboxyl group of cysteine is deprotonated in buffer solution while the amine group is still protonated, AuNPs aggregation occurs through electrostatic interaction between cysteine-bound AuNPs. In contrast, in the presence of Cu^{2+}, Cu^{2+} can catalyze oxidation of cysteine to quickly form disulfide cystine by H_2O_2. With an increase in the concentration of Cu^{2+}, the cysteine-induced aggregation of AuNPs decreased. The aggregation degree of AuNPs can be indicated by using the catalysis of Cu^{2+} toward the oxidation reaction of H_2O_2–cysteine as an amplifier system, thus providing a way for qualitatively/quantitatively detecting the Cu^{2+} level by monitoring the change in the colorimetric signal (the color/absorbance of AuNPs).

2. Experimental

Chemicals and apparatus

Hydrogen tetrachloroaurate(III) dehydrate ($HAuCl_4 \cdot 4H_2O$), citric acid ($C_6H_8O_7$), trisodium citrate dihydrate ($Na_3C_6H_5O_7 \cdot 2H_2O$), polyethylene glycol (PEG; molecular weight: 10 000), H_2O_2 (30 wt%), KNO_3, $HgSO_4$, KCl, $Fe(NO_3)_2$, $Fe(NO_3)_3$, $MgCl_2$, and other chemicals were all obtained from Sinopharm Chemical Reagent Co., Ltd (Shanghai, China). All chemicals used were of analytical grade. Unless otherwise noted, distilled water was used throughout the course of the investigation. The room temperature at which the work was conducted was 25 °C. The working solutions of Cu^{2+} were freshly prepared by dilution from the $CuSO_4$ stock solution (0.1 M). Cysteine stock solution (1 mM) was freshly prepared and used up within seven days of storage. Both the $CuSO_4$ and cysteine stock solutions were stored at 4 °C. The $C_6H_8O_7$–$Na_3C_6H_5O_7$ buffer solution (100 mM, pH 5.0) was prepared by dissolving $C_6H_8O_7$ (0.861 g) and $Na_3C_6H_5O_7 \cdot 2H_2O$ (1.735 g) in water (100 mL). UV-vis spectra were measured on a Shimadzu UV-2550 UV-vis spectrophotometer operated at a resolution of 0.5 nm. Photographs were taken using a digital camera.

Synthesis of AuNPs

Citrate-capped AuNPs were prepared according to the Frens method.[23] In brief, 100 mL aqueous solution of $HAuCl_4 \cdot 4H_2O$ (0.01%) was rapidly heated to boiling under vigorous stirring in a three-necked flask. Then 1 mL of trisodium citrate dihydrate solution (1%) was quickly added, resulting in the change of solution color from pale yellow to deep red. After the color change, the solution was heated for an additional 30 min for complete reduction of the Au(III) ions. The maximum absorption wavelength of the AuNPs, which was measured by UV-vis spectrophotometer, was 520 nm. Finally, 100 mL of the AuNPs was mixed with 1.25 mL of 0.1 g mL^{-1} PEG (molecular weight: 10 000) to yield well-dispersed AuNPs. The resulting as-prepared AuNPs was addressed as PEG-AuNPs.

Cu^{2+} detection

Typically, an aliquot of a solution of cysteine (150 μL; 100 μM) was placed separately in centrifuge tube, into which 300 μL of $C_6H_8O_7$–$Na_3C_6H_5O_7$ buffer solution (100 mM, pH 5.0), H_2O_2 (50 μL; 12 mM) and different concentrations of Cu^{2+} (100 μL) were added. The total volume of the mixture solution was 600 μL, and the final concentrations of cysteine, buffer and H_2O_2 were 25 μM, 50 mM and 1 mM, respectively. The mixtures were equilibrated at room temperature for 10 min. Afterwards, the solution was sequentially added with 2400 μL of PEG-AuNPs. Although the change of color was instant, 5 min was allowed for the full colorimetric response, which was then measured with the naked eye or with UV-vis spectroscopy at room temperature.

3. Results and discussion

General principle for the detection of Cu^{2+}

The principle of the Cu^{2+} colorimetric sensor is illustrated in Scheme 1. The as-prepared PEG-AuNPs is stable in the aqueous solution. Before adding the buffer solution, the AuNPs were first stabilized with PEG. Fig. S1† shows that the maximum absorbance of PEG-AuNPs with the addition of H_2O_2 and buffer solution appears at 520 nm, and the absorbance of the solution at 520 nm almost remains the same contrasted to AuNPs, indicating that they were well dispersed. Since cysteine could stimulate the aggregation of PEG-AuNPs through the formation of inter-particle H-bonds and zwitterionic electrostatic interactions.[21,24] Accordingly, rapid aggregation proceeds leading to a color change from the red color of the individual AuNPs to the blue color corresponding to the aggregated AuNPs. The aggregation was also reflected in the UV-vis spectrum of the AuNPs, with the decrease in absorption at 520 nm and the production of a new absorption peak at 650 nm (Fig. 1b). The oxidation of cysteine to cystine by H_2O_2 is a slow process.[25] As can be seen from Fig. 1d, with the addition of cysteine and H_2O_2, there is almost no obvious change of the plasmon band of the PEG-AuNPs contrasted to that aggregated individually by cysteine. However, this reaction could be dramatically catalyzed in the presence of Cu^{2+}. The Cu^{2+}-catalyzed oxidation of cysteine by

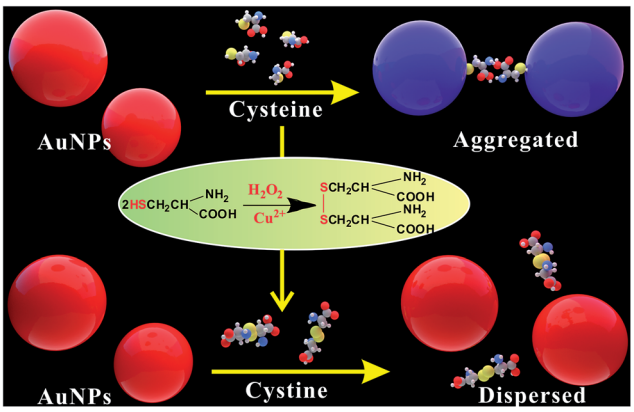

Scheme 1 Schematic representation of the colorimetric detection of Cu^{2+}.

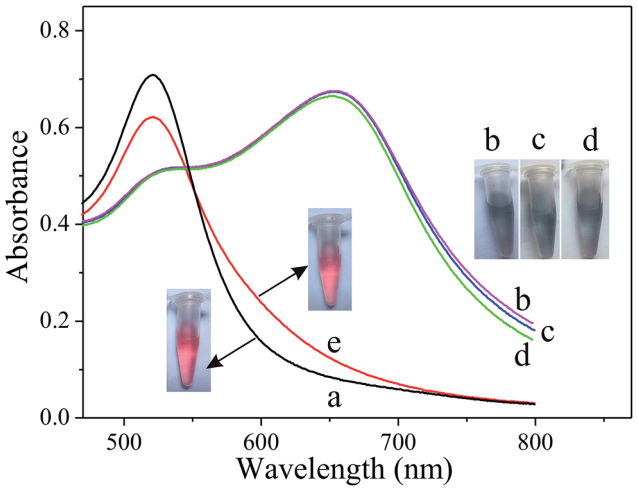

Fig. 1 UV-vis spectra of (a) PEG-AuNPs, (b) PEG-AuNPs + cysteine (25 μM), PEG-AuNPs containing the mixtures of (c) cysteine (25 μM) + Cu^{2+} (2 μM), (d) cysteine (25 μM) + H_2O_2 (1 mM) and (e) cysteine (25 μM) + H_2O_2 (1 mM) + Cu^{2+} (2 μM). The inset photographic images are the corresponding colorimetric response.

H_2O_2 can yield cystine. The resulting disulfide does not stimulate any aggregation of the PEG-AuNPs. Thus, the aggregation role of cysteine is deactivated by Cu^{2+}. Therefore, Cu^{2+} could be readily detected through monitoring the color change of PEG-AuNPs solution by just naked eye. Since the color change of the PEG-AuNPs is directly dependent on the Cu^{2+} concentration, the sensing system can serve as a colorimetric probe for the quantitative detection of Cu^{2+}.

Optimization of assay conditions

As illustrated in Fig. 2, the as-prepared PEG-AuNPs nanodispersion exhibits wine-red color and shows a strong absorbance band at 520 nm in the UV-vis absorption spectrum. The addition of cysteine to the PEG-AuNPs led to an observable aggregation of the AuNPs, and the solution color turned from the original wine red to purple then to blue. We also noticed that the color of PEG-AuNPs remained blue with the addition of cysteine concentration from 25 to 50 μM. In the corresponding UV-vis spectra (Fig. 2a), with the increase of cysteine concentration the intensity of the absorption band at 520 nm decreased systematically accompanied with the appearance of a new absorption band at 650 nm, which originates from the interparticle coupled plasmon absorbance of the aggregated AuNPs. The absorbances at 650 and 520 nm are related to the amounts of aggregated and dispersed AuNPs, respectively. So, the ratio of the absorbance at 650 nm to that at 520 nm (A_{650}/A_{520}) was used to express the molar ratio of aggregated to dispersed AuNPs. As shown in Fig. 2b, the abscissa denotes the concentration of cysteine, and the ordinate denotes the relative absorbance value of the PEG-AuNPs with the addition of cysteine. The A_{650}/A_{520} of PEG-AuNPs increased with the increase of cysteine. When the concentration of cysteine is higher than 25 μM, no obvious change can be observed for the value of A_{650}/A_{520}. Evidently, the aggregation of the AuNPs reaches a constant saturation value at a cysteine concentration of 25 μM. Since, improvement in the sensitivity of the Cu^{2+} detection relies on a decrease in the amount of cysteine used. Therefore, we selected 25 μM of cysteine concentration as the optimal concentration for further experiments.

In our study, the as-prepared AuNPs were capped with citrate. Ionic strength of solution exerts a strong effect on the interaction between citrate-coated AuNPs. We first tested the stability of citrate-capped AuNPs. Fig. S2a† shows the ratio of A_{650}/A_{520} of AuNPs in the presence of NaCl. Initially, the AuNPs with citrate as the stabilizer appeared red in color. After NaCl was added, the AuNPs were stable in <50 mM NaCl. With a increase in salt concentration (*e.g.*, >100 mM NaCl), the electrostatic repulsion between negatively charged (citrate) AuNPs was screened, resulting in the aggregation of AuNPs with a red-to-blue colour change. Accordingly, the A_{650}/A_{520} increases, which indicates the aggregation of AuNPs. However, this aggregation could be efficiently inhibited with the prior addition of PEG to a dispersion of AuNPs. With a few percent of PEG, AuNPs are stable even under extreme conditions such as with very high salt and extreme pH values.[26,27] Therefore, PEG is a suitable polymer surfactant employed in our experiment. In

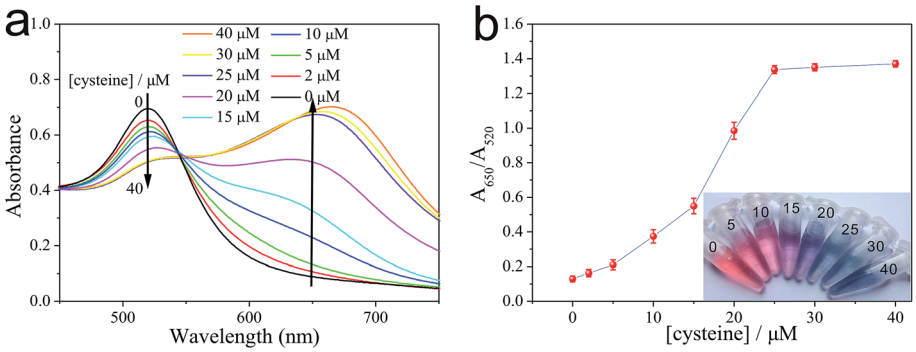

Fig. 2 (a) Absorption spectra corresponding to the PEG-AuNPs containing different concentrations of cysteine in buffer and H_2O_2. (b) Effect of cysteine concentration on the value of A_{650}/A_{520} of the PEG-AuNPs-based detection system. Error bars derived from a set of three experiments. The inset photographic images displays that the aggregation of PEG-AuNPs induced by different concentrations of cysteine. The cysteine concentrations in μM are listed at the top of the respective solutions.

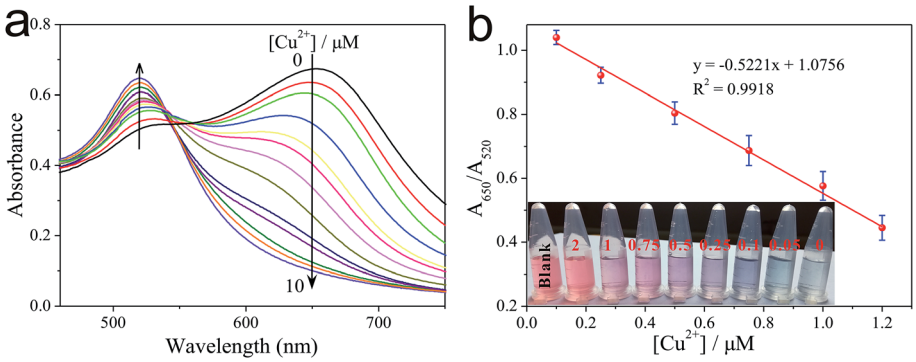

Fig. 3 (a) UV-vis absorption spectra of PEG-AuNPs in the presence of a series of concentrations of Cu^{2+}. From top to ground, the concentrations of Cu^{2+} are 0 μM, 0.05 μM, 0.1 μM, 0.25 μM, 0.5 μM, 0.75 μM, 1.0 μM, 1.2 μM, 1.5 μM, 2.0 μM, 3.0 μM, 5.0 μM and 10 μM, respectively. (b) Linear fitting curve of the A_{650}/A_{520} value *versus* the concentrations of Cu^{2+} from 0.1 μM to 1.2 μM. The scale bars represent the standard deviations of three replicated samples. Naked-eye observation of different concentrations of Cu^{2+} was shown in the inset. The Cu^{2+} concentrations, in μM, are listed at the top of the respective solutions.

our study, the addition of only 0.125% PEG caused no aggregation of AuNPs with increasing the amount of NaCl up to 200 mM (Fig. S2b†). The results indicated that the PEG-stabilized AuNPs were significantly more stable than citrate-coated AuNPs. Nevertheless, at relatively high concentrations of PEG, the adsorption of cysteine on the surface of AuNPs would decrease, reducing the degree of AuNPs aggregation. Fig. S3† shows the absorption ratio of AuNPs stabilized by different concentrations of PEG in the presence of 25 μM cysteine. When PEG concentration is below 0.125%, the high ratio of A_{650}/A_{520} indicates aggregated AuNPs because that low concentrations of PEG have a moderate protection. However, when the concentration of PEG is higher than 0.125%, the A_{650}/A_{520} decreased sharply, because the AuNPs aggregate induced by cysteine was significantly alleviated. Since, the more PEG was added, the more cysteine was needed to produce aggregation of AuNPs completely. In view of the sensing effect of our detection system, the PEG concentration was fixed at 0.125% for the subsequent experiments.

The reaction time of the proposed assay was examined and is shown in Fig. S4.† It can be seen that A_{650}/A_{520} decreases gradually during the first 10 min. This result is consistent with the fact that cysteine could be effectively oxidized to cystine by H_2O_2 in the presence of Cu^{2+}. Thus, the cysteine-stimulated aggregation of the AuNPs would be prohibited. However, in the presence of different concentrations of Cu^{2+}, especially 2 μM Cu^{2+}, the A_{650}/A_{520} value nearly reaches a plateau after incubation for 10 min. Therefore, to quantitatively analyze the Cu^{2+} concentration, 10 min was chosen as the reaction time in the experiments.

The cysteine-induced aggregation of PEG-AuNPs should be at an appropriately pH. Then, the pH of the solution needs to be optimized so that the influence on the stability of the PEG-AuNPs and the background agglomeration would be minimal. Accordingly, the effect of pH to the value of A_{650}/A_{520} was investigated. The experiment was performed in the 3.5–6.5 pH range obtained by adjusting the ratio of $C_6H_8O_7$ to $Na_3C_6H_5O_7$. The reaction conditions were the same as those of the typical assay except the varied factors that we should explore, and the concentration of cysteine was fixed at 25 μM. As shown in Fig. S5,† the values of A_{650}/A_{520} at pH 5.0 reach maximum whether there have Cu^{2+} or not, which illustrates that pH has effective influence on the aggregation of PEG-AuNPs induced by cysteine. This is possibly due to various ionic forms of cysteine that are highly related to the pH. The isoelectric point (pI_0) of cysteine is reported as 5.02.[28,29] When pH is at approximate 5.02, the dominant form of cysteine in the solution is zwitterionic, meaning that the cysteine molecules can combine with each other through a two-point electrostatic interaction and induce the maximum aggregation of AuNPs. Consequently, the pH at 5.0 was chosen in our experiments.

The prerequisite for the successful use of AuNPs as an analytical probe is their colloidal stability. Then, the concentration of buffer solution was optimized. As shown in Fig. S6,†

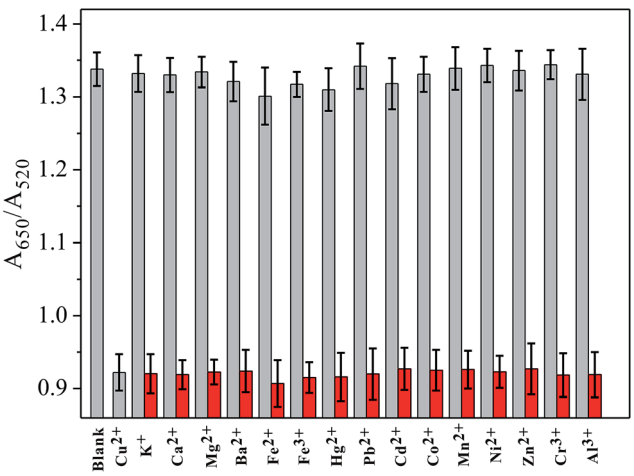

Fig. 4 Absorbance ratios of PEG-AuNPs when different kinds of foreign ions were added alone and along with Cu^{2+}. Gray bars represent the addition of single metal ion; red bars are the addition of Cu^{2+} with another metal ion. The concentration of Cu^{2+} was 250 nM, and other metal ions were all 5.0 μM.

Table 1 Determination of Cu^{2+} in water samples

Sample	Detected/μM	Added/μM	Detected/μM	RSD (%)	Recovery (%)
Ground water	Undetectable				
1		0.2	0.18	3.6	90
2		0.5	0.53	4.1	106
3		1.0	1.07	5.6	107
Tap water	Undetectable				
1		0.2	0.19	3.0	95
2		0.5	0.51	4.3	102
3		1.0	1.05	4.9	105

when $C_6H_8O_7$–$Na_3C_6H_5O_7$ solution was used as the reaction buffer, PEG-AuNPs were well dispersed at buffer concentrations <50 mM. Nevertheless, when the buffer concentrations were >50 mM, the A_{650}/A_{520} of PEG-AuNPs increased significantly with the increase of buffer concentration, indicating that PEG-AuNPs began to aggregate. Therefore, 50 mM buffer was chosen as the optimum buffer condition.

Next, the effect of concentration of H_2O_2 was investigated over the range from 0 to 10 mM. As shown in Fig. S7,† when H_2O_2 concentrations were <1 mM, the ratios of A_{650}/A_{520} clearly decrease with increasing concentration of H_2O_2. This result is consistent with the fact that cysteine is effectively oxidized to cystine by H_2O_2 (in the presence of Cu^{2+}), thus, prohibiting the cysteine-stimulated aggregation of the PEG-AuNPs. Evidently, the rate of the redox reaction would accelerate with the elevated amounts of H_2O_2. However, the A_{650}/A_{520} value almost reaches a plateau when H_2O_2 concentrations were >1 mM, indicating that the reaction rate became a constant saturation with the addition of 1 mM H_2O_2 in the cysteine/Cu^{2+} reaction mixture for a fixed time-interval of 10 min, and hence all other experiments were conducted under this condition.

Detection of Cu^{2+}

Under the optimized conditions, cysteine was reacted with different concentrations of Cu^{2+} in the presence of H_2O_2 and buffer for a time-interval of 10 min, and afterwards the reaction mixture was incubated with PEG-AuNPs reporter system for a further 5 min. The corresponding colors of the solutions with different concentrations of Cu^{2+} are shown in Fig. 3b. We can observe a gradually blue-to-red color change when the concentration of Cu^{2+} increased from 0 to 2.0 μM. The detection limit of Cu^{2+} was 250 nM. This result demonstrates that the proposed method could be used for the direct detection of Cu^{2+} with the naked eye. To evaluate the minimum concentration of Cu^{2+} that can be detected by this colorimetric method, UV-vis spectroscopy was used to quantitatively determine the concentration of Cu^{2+}. As the concentration of Cu^{2+} increase, more cysteine could be oxidized by H_2O_2. So the aggregation process of PEG-AuNPs would be inhibited and correspondingly the ratio of A_{650}/A_{520} decreased. Fig. S8† shows the Cu^{2+}-dependent changes of the A_{650}/A_{520} values, which correspond to the spectra in Fig. 3a. By monitoring the absorbance ratio of A_{650}/A_{520}, an appropriate calibration curve relating to the absorbance of the aggregated PEG-AuNPs with the concentration of Cu^{2+} was derived. The calibration curve was linear in the range from 0.1 to 1.2 μM and fit the linear equation $y = -0.5221x + 1.0756$ ($R^2 = 0.9918$). The detection limit of Cu^{2+} was 0.05 μM (Fig. 3a), which is lower than the maximum allowable level of Cu^{2+} in drinking water (20 μM; 1.3 ppm) set by the United States Environmental Protection Agency (EPA).[30] The ability of the sensor for detection of Cu^{+}, another oxidation state of copper, is discussed in Fig. S9, ESI.†

To investigate the selectivity of the sensor toward Cu^{2+}, other metal ions, including K^{+}, Ca^{2+}, Mg^{2+}, Ba^{2+}, Fe^{2+}, Fe^{3+}, Hg^{2+}, Pb^{2+}, Cd^{2+}, Co^{2+}, Mn^{2+}, Ni^{2+}, Zn^{2+}, Cr^{3+} and Al^{3+} (all 5 μM), were examined. Under typical experiment conditions, one of these metal ions was added alone or together with Cu^{2+} (250 nM) to the cysteine solution in the presence of H_2O_2 for a 10 min reaction time, and then incubated with PEG-AuNPs for a further 5 min. As shown in Fig. 4, no noticeable interference for the detection of Cu^{2+} was observed, indicating that the sensor responded selectively toward Cu^{2+} by a factor of over 20-fold relative to the other metal ions. The excellent selectivity of this sensor could be attributed to the great specificity of the oxidation reaction to the catalysis of Cu^{2+}. It has been reported that Cu^{2+}-catalyzed oxidation of cysteine can be inhibited by iron salts.[31] However, in our assay, control experiments revealed that iron salts could not affect the detection of Cu^{2+} (for more details, see Fig. S10 in ESI†).

Real sample tests

To further investigate the feasibility and possible application of the developed assay for analysis of Cu^{2+} in real samples, the detection of Cu^{2+} in ground water and tap water was carried out. No signal was observed for Cu^{2+} when unspiked water samples were analyzed, so they were spiked with three levels of Cu^{2+} (0.2 μM, 0.5 μM, 1.0 μM) and analyzed. The UV-vis spectra of the probing system for the detection of Cu^{2+} in real samples is discussed in Fig. S11, ESI.† As shown in Table 1, the average recoveries ranged between 90% and 107%, with the relative standard deviations were less than 6% ($n = 3$). The results demonstrated the potential application of this method for the determination of Cu^{2+} in practical sample analysis.

4. Conclusion

In conclusion, the present study has developed a sensitive method for the detection of Cu^{2+} through the aggregation of PEG-AuNPs by the cysteine/H_2O_2 reporter system. In the

presence of H_2O_2, Cu^{2+} exhibited high catalytic ability on oxidation reaction of cysteine which could modulate the plasmonic signals of PEG-AuNPs. Naked-eye-based colorimetric assay and UV-vis absorption spectroscopic method were able to sensitively detect Cu^{2+} in water. No significant interference of commonly encountered metal ions to Cu^{2+} detection was found, proving the assay presented in this paper is highly selective. This simple and cost-effective system appears to hold great practical potential for sensitive and selective detection of Cu^{2+} in real samples.

Conflicts of interest

There are no conflicts to declare.

Acknowledgements

This research was supported by the Science and Technology Development Program of Henan (172102210207), the Doctor Foundation of Henan Institute of Engineering (D2014016), the National Natural Science Foundation of China (51608175), the Natural Science Foundation of Anhui Province (1708085ME96) and the Key Natural Science Research Project for Colleges and Universities of Anhui Province (KJ2016A638).

References

1 K. J. Barnham, C. L. Masters and A. I. Bush, *Nat. Rev. Drug Discovery*, 2004, **3**, 205–214.
2 D. W. Domaille, E. L. Que and C. J. Chang, *Nat. Chem. Biol.*, 2008, **4**, 168–175.
3 J. Huang, S. Bai, G. Yue, W. Cheng and L. Wang, *RSC Adv.*, 2017, **7**, 28556–28563.
4 H. Zhang, R. Fan, W. Chen, J. Fan, Y. Dong, Y. Song, X. Du, P. Wang and Y. Yang, *Cryst. Growth Des.*, 2016, **16**, 5429–5440.
5 C. Zou, M. F. Foda, X. Tan, K. Shao, L. Wu, Z. Lu, H. S. Bahlol and H. Han, *Anal. Chem.*, 2016, **88**, 7395–7403.
6 S. Wang, C. Liu, G. Li, Y. Sheng, Y. Sun, H. Rui, J. Zhang, J. Xu and D. Jiang, *ACS Sens.*, 2017, **2**, 364–370.
7 R. S. Weatherup, B. Eren, Y. Hao, H. Bluhm and M. B. Salmeron, *J. Phys. Chem. Lett.*, 2016, **7**, 1622–1627.
8 J. S. Becker, A. Matusch, C. Depboylu, J. Dobrowolska and M. V. Zoriy, *Anal. Chem.*, 2007, **79**, 6074–6080.
9 P. Ndokoye, J. Ke, J. Liu, Q. Zhao and X. Li, *Langmuir*, 2014, **30**, 13491–13497.
10 M. Vázquez-González, W.-C. Liao, R. Cazelles, S. Wang, X. Yu, V. Gutkin and I. Willner, *ACS Nano*, 2017, **11**, 3247–3253.
11 I. Ibrahim, H. N. Lim, O. K. Abou-Zied, N. M. Huang, P. Estrela and A. Pandikumar, *J. Phys. Chem. C*, 2016, **120**, 22202–22214.
12 Q. Gao, Y. Zheng, C. Song, L. Q. Lu, X. K. Tian and A. W. Xu, *RSC Adv.*, 2013, **3**, 21424–21430.
13 V. N. Mehta and S. K. Kailasa, *RSC Adv.*, 2015, **5**, 4245–4255.
14 Y. J. Ye, M. X. Lv, X. Y. Zhang and Y. X. Zhang, *RSC Adv.*, 2015, **5**, 102311–102317.
15 Z. Hu, M. Xie, D. Yang, D. Chen, J. Jian, H. Li, K. Yuan, Z. Jiang and H. Zhou, *RSC Adv.*, 2017, **7**, 34746–34754.
16 Y. J. Ye, Y. Guo, Y. Yue and Y. X. Zhang, *Anal. Methods*, 2015, **7**, 4090–4096.
17 Y. Zhou, S. Wang, K. Zhang and X. Jiang, *Angew. Chem., Int. Ed.*, 2008, **47**, 7454–7456.
18 W. Qu, Y. Liu, D. Liu, Z. Wang and X. Jiang, *Angew. Chem., Int. Ed.*, 2011, **50**, 3442–3445.
19 S. Wang, X. Wang, Z. Zhang and L. Chen, *Colloids Surf., A*, 2015, **468**, 333–338.
20 H. M. Kao, P. J. Chiu, G. L. Jheng, C. C. Kao, C. T. Tsai, S. L. Yau, H. H. G. Tsai and Y. K. Chou, *New J. Chem.*, 2009, **33**, 2199–2203.
21 C. H. Lu, Y. W. Wang, S. L. Ye, G. N. Chen and H. H. Yang, *NPG Asia Mater.*, 2012, **4**, e10.
22 Y. J. Ye, Y. Guo, Y. Yue, H. J. Huang, L. T. Zhao, Y. M. Gao and Y. X. Zhang, *Anal. Methods*, 2015, **7**, 566–572.
23 G. Frens, *Nat. Phys.*, 1973, **241**, 20–22.
24 M. N. Bui, S. Ahmed and A. Abbas, *Nano Lett.*, 2015, **15**, 6239–6246.
25 F. Wang, X. Q. Liu, C. H. Lu and I. Willner, *ACS Nano*, 2013, **7**, 7278–7286.
26 X. Zhang, M. R. Servos and J. Liu, *J. Am. Chem. Soc.*, 2012, **134**, 9910–9913.
27 N. J. Lang, B. Liu, X. Zhang and J. Liu, *Langmuir*, 2013, **29**, 6018–6024.
28 H. Huang, X. Liu, T. Hu and P. K. Chu, *Biosens. Bioelectron.*, 2010, **25**, 2078–2083.
29 P. K. Sudeep, S. T. S. Joseph and K. G. Thomas, *J. Am. Chem. Soc.*, 2005, **127**, 6516–6517.
30 J. Liu and Y. Lu, *J. Am. Chem. Soc.*, 2007, **129**, 9838–9839.
31 R. Munday, C. M. Munday and C. C. Winterbourn, *Free Radical Biol. Med.*, 2004, **36**, 757–764.